

# Extracting Coupling Coefficients of Directional Couplers.

Umar Khan<sup>1,2</sup>, Yufei Xing<sup>1,2</sup>, Antonio Ribeiro<sup>1,2</sup>, Wim Bogaerts<sup>1,2</sup>

<sup>1</sup>Ghent University - imec, Technologiemark 126, 9052 Ghent, Belgium

<sup>2</sup>Center for Nano- and Biophotonics, Ghent University, Belgium

e-mail: Umar.Khan@ugent.be

## ABSTRACT

We experimentally demonstrate the extraction of dispersive directional coupler parameters (coupling coefficients) using optical transmission measurements. The coupling coefficients are extracted using both direct transmission of directional couplers and through more complex *Mach-Zehnder interferometers* (MZI) and we conclude that coefficients using the MZI circuits give better accuracy.

**Keywords:** silicon photonics, directional couplers, parameter extraction, coupling coefficients, behavioral model, spectrum fitting.

## 1 INTRODUCTION

The *directional coupler* (DC) is a four-port reciprocal passive optical device frequently used for splitting and combining of optical power in ring resonators, *Mach-Zehnder Interferometers* (MZI) and optical filters. In a DC, two optical waveguides are brought so close to each other that light starts coupling evanescently. This evanescent coupling is sensitive to changes in geometrical parameters i.e. the gap between the waveguides and waveguide cross-sections. This is especially true in high-contrast silicon photonics, where the coupling parameters become quite wavelength dependent, and nanometer-level change in geometrical parameters due to fabrication variations can result into noticeably different power coupling. Such deviations will propagate and accumulate in circuits (especially filter circuits) and deteriorate the overall circuit performance[1]. Given both the importance of the component and its sensitivity, a method to accurately extract the coupling of a fabricated DC is very useful. In this research, we experimentally demonstrate the extraction of coupling coefficients of fabricated DCs using transmission measurements on two different methods, i.e. the 'naked' DC and an MZI with embedded DCs, and compare the accuracy of these two methods.

## 2 EXTRACTION OF COUPLING COEFFICIENTS

The coupling coefficients of DC can be extracted using different approaches [2] but in this research we focus on extraction by the fitting of the measured optical spectrum to a dispersive behavioural model. A *coupled mode theory* (CMT) based behavioural model for the DC [3] is summarized in Fig. 1a. In this model, the coupling in a DC is divided into two contributions, i.e. a length dependent field coupling  $\kappa'(\lambda)$  in the straight section and the length independent 'lumped' coupling  $\kappa_0(\lambda)$  in the bend sections. The wavelength dependence of these coupling coefficients is captured in a second order polynomial expansion:

$$\kappa'(\lambda) = \kappa'(\lambda_0) + (\lambda - \lambda_0) \frac{\partial \kappa'}{\partial \lambda} + (\lambda - \lambda_0)^2 \frac{\partial^2 \kappa'}{\partial \lambda^2} \quad (1)$$

$$\kappa_0(\lambda) = \kappa_0(\lambda_0) + (\lambda - \lambda_0) \frac{\partial \kappa_0}{\partial \lambda} + (\lambda - \lambda_0)^2 \frac{\partial^2 \kappa_0}{\partial \lambda^2} \quad (2)$$

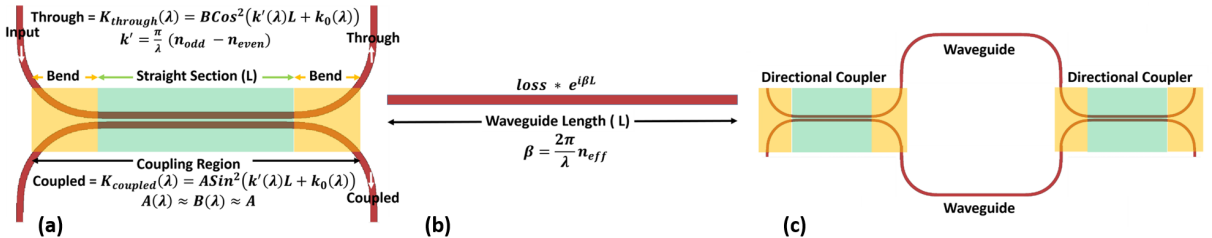


Figure 1. (a) The behavioral model for the directional coupler. Coupling length dependent power coupling in the straight section is represented as  $\kappa'$ . The coupling in the bend sections which is independent of the coupling length is represented as  $\kappa_0$ . The field coupling  $\kappa'$  is determined by the difference between the even and odd modes in the coupling section. (b) The behavioral model for a straight waveguide. Waveguide loss, effective index ( $n_{eff}$ ) and group index ( $n_g$ ) are the model parameters. (c) An MZI consisting of directional couplers and waveguides can be simulated using the behavioral models for couplers and waveguides.

We have neglected the higher order terms as they do not add much to the extraction accuracy but do complicate the fitting process. The behavioural model was implemented in the circuit simulator CAPHE from Luceda Photonics[4]. This model has six model parameters to be fitted, i.e.  $\kappa'$ ,  $\frac{\partial \kappa'}{\partial \lambda}$ ,  $\frac{\partial^2 \kappa'}{\partial \lambda^2}$ ,  $\kappa_0$ ,  $\frac{\partial \kappa_0}{\partial \lambda}$  and  $\frac{\partial^2 \kappa_0}{\partial \lambda^2}$ .

The MZI circuit consists of a splitter, a combiner and two waveguide arms that connect the splitter to the combiner, Fig. 1c. For the waveguide arms the model has two parameters: the effective index  $n_{eff}$  and the group  $n_g$  index at a reference wavelength  $\lambda_0$ , shown in Fig. 1b. This results in first-order wavelength dispersion of the effective index:

$$n_{eff}(\lambda) = n_{eff} - (\lambda - \lambda_0) \cdot \frac{n_g - n_{eff}}{\lambda_0} \quad (3)$$

So, fitting the MZI spectrum introduces two additional model parameters ( $n_{eff}$  and  $n_g$ ) on top of the six DC model parameters. The extraction using both the naked DC and the MZI circuit is explained below.

## 2.1 Extraction using 'Naked' Directional Couplers

DCs of different coupling lengths with same waveguide cross-sections ( $0.45\mu m \times 0.22\mu m$ ), coupling gaps ( $0.25\mu m$ ) and a bend radius of  $5\mu m$  were designed to extract the field ( $\kappa'$ ) and lumped ( $\kappa_0$ ) coupling coefficients. Cross-sections, coupling gaps and bending radius were kept same to keep coupling coefficients same for all the devices. The coupling lengths were varied to separate the contributions from the straight and the bend sections, as a measurement of a single coupling length cannot distinguish between the two. Designed devices were fabricated using e-beam lithography through the Australian Silicon Photonics prototyping service at RMIT Melbourne. Please note that fabricated devices were air-clad from the top.

Fabricated DCs were optically measured using a tunable laser and a photo-detector in a clean-room environment. Measured spectra of four devices with coupling lengths of 10, 20, 30 and 40  $\mu m$  were fitted simultaneously to the CAPHE model shown in Fig. 1a using the *non-linear least-squares minimization and curve-fitting* (lmfit) tool for Python. The fitting was performed for same field ( $\kappa'$ ) and lumped ( $\kappa_0$ ) coupling coefficients as bending radii, cross-sections and coupling gaps were the same for all the fitted devices. The measured and the fitted spectra are shown in Fig. 2c below. Ideally, two spectra can also be used for fitting but we have used four for increased robustness and accuracy. The accuracy can further be improved by fitting both through and cross ports simultaneously. The extracted dispersive coupling coefficients are shown in Fig. 2a and 2b. It can be noticed that the coupling coefficients increase with increasing wavelength according to our expectations.

## 2.2 Extraction using Mach-Zehnder Interferometers

We designed MZI circuits having the same DC as splitter and combiner to extract the coupling coefficients. Again, we used circuits with couplers of different lengths keeping waveguide cross-sections ( $0.45\mu m \times 0.22\mu m$ ), coupling gap ( $0.3\mu m$ ) and bend radius ( $5\mu m$ ) the same. The differential delay length ( $\Delta L$ ) between arms of the MZI was designed to be 150  $\mu m$  to have multiple resonance features within the measurement range ( $1.5\mu m - 1.59\mu m$ ) for increased fitting accuracy. Fabrication imperfections were taken into account while generating the layout of the designed MZI structures, Figure 3a. The couplers and waveguide arms were kept as close to each other as possible to make them less prone to fabrication variations. These MZI devices were fabricated using the imec passive silicon photonics process through the Europractice *multi-project wafer* (MPW) service. It should be mentioned here that fabricated devices have a silica ( $SiO_2$ ) top cladding in contrast to air top cladding for DCs fabricated by the e-beam lithography. The gap between the waveguides was chosen to be 0.3  $\mu m$  instead of 0.25  $\mu m$  in order to somewhat compensate the effect of this cladding difference.

The fabricated MZI devices were optically measured using the tunable laser and a photo-detector in a clean-room environment. The measured spectra for three MZI structures having DCs of coupling lengths 1.0, 7.3 and 36.1  $\mu m$  were simultaneously fitted to the CAPHE circuit model using the above mentioned lmfit tool to

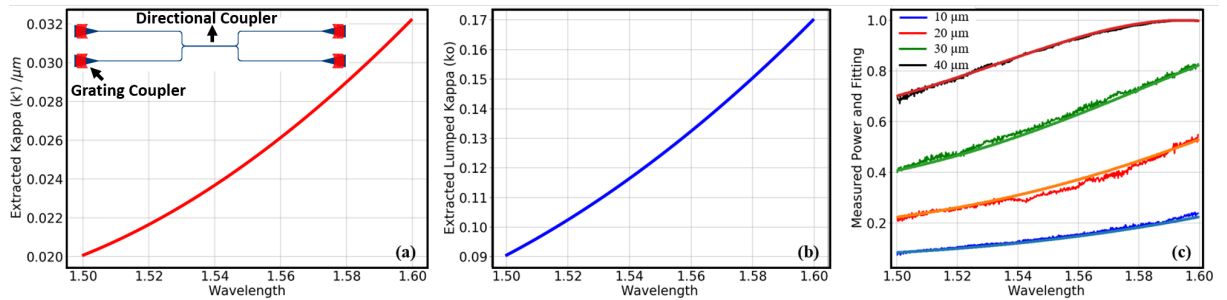


Figure 2. (a) Extracted field coupling coefficient using a 'naked' directional coupler. (b) Extracted lumped coupling coefficient. (c) Measured and the fitted spectra from the coupled port of the directional couplers with coupling lengths of 10, 20, 30 and 40  $\mu m$ .

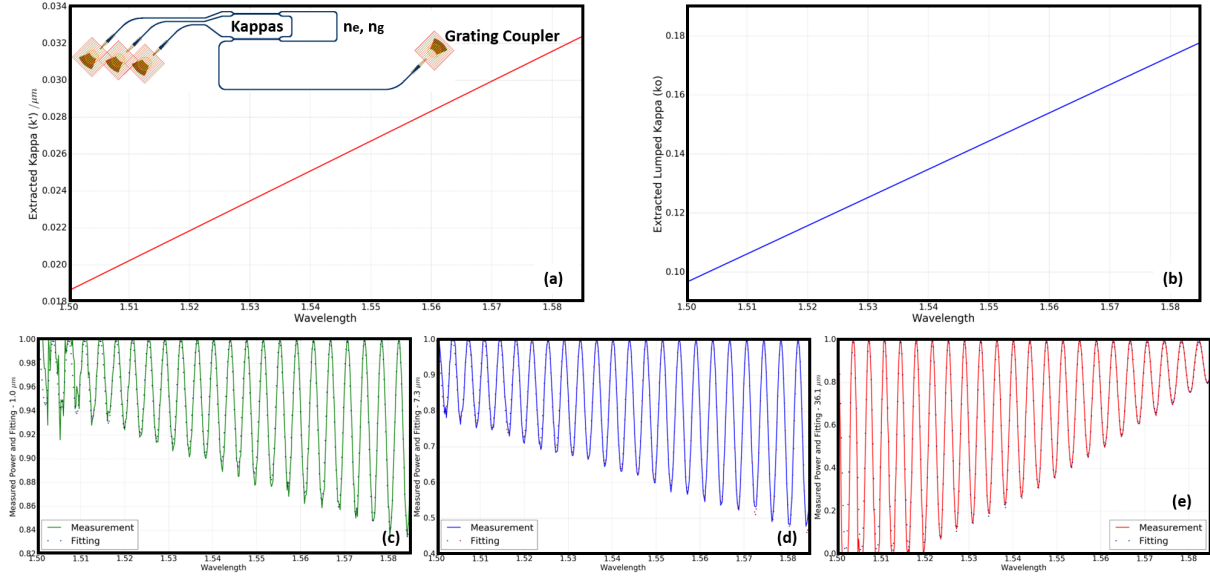


Figure 3. (a) Extracted field coupling coefficients ( $\kappa'$ ) from the MZI. (b) Extracted lumped coupling coefficient ( $\kappa_0$ ). (c,d,e) Measured and the fitted spectra from the coupled spectra of the MZI structures with coupling lengths 7.3, 36.1 and 1.0  $\mu\text{m}$  respectively.

extract six coupler related ( $\kappa'$ ,  $\frac{\partial \kappa'}{\partial \lambda}$ ,  $\frac{\partial^2 \kappa'}{\partial \lambda^2}$ ,  $\kappa_0$ ,  $\frac{\partial \kappa_0}{\partial \lambda}$  and  $\frac{\partial^2 \kappa_0}{\partial \lambda^2}$ ) and two waveguide related ( $n_{eff}$  and  $n_g$ ) model parameters. Effective and group indices of both MZI arms were considered to be same for these extractions neglecting the fabrication variability. The fitted and the measured spectra for the used MZI devices are shown in Fig. 3c-e. Good fitting of the spectra confirm that fabrication variability has not dramatically affected the circuit, thanks to the compact layout. The wavelength dependent field ( $\kappa'$ ) and lumped ( $\kappa_0$ ) coupling coefficients are shown in Fig. 3a and 3b, respectively. The effective and group indices were extracted to be 2.33 and 4.23. The extracted coupling coefficient values increase with increasing wavelength and values are comparable to the values extracted for the DCs fabricated by e-beam lithography. This shows our design assumption that the effect of the cladding difference can be compensated by a larger coupling gap. The extraction errors for MZI devices were found to be smaller than the extractions from the directional couplers due to larger number of features within the measurement range.

### 3 CONCLUSIONS

We demonstrated experimental extraction of wavelength dependent field and lumped coupling coefficients using two different fabricated structures. The extraction was carried out by fitting of the measured spectra to the behavioral models to the transmission of a 'naked' DC and an MZI circuit. The MZI-based extraction not only provides the wavelength dependent coupling coefficients with higher accuracy and smaller errors but on top of that extracts the effective and the group indices of the waveguides. This is due to the fact that the extraction in the MZI spectra is based on the extinction ratio of the spectral features rather than the absolute power measurements which are susceptible to variations from the measurement setup (e.g. fiber alignment).

### ACKNOWLEDGMENT

This work is supported by the Flemish Agency for Innovation and Entrepreneurship (VLAIO) with the MEPIC project.

### REFERENCES

- [1] W. Bogaerts, U. Khan, and Y. Xing, "Layout-Aware Yield Prediction of Photonic Circuits," in IEEE International Conference on Group IV Photonics, Mexico, pp. 93-94, 2018.
- [2] W. Bogaerts, P. De Heyn, T. Van Vaerenbergh, K. De Vos, S. Selvaraja, T. Claes, P. Dumon, P. Bienstman, D. Van Thourhout, and R. Baets, "Silicon microring resonators," Laser Photonics Rev. 6(1), pp 47-73, 2012.
- [3] Y. Xing, U. Khan, A. R. Alves Júnior, and W. Bogaerts, "behavioral model for directional coupler," in Proceedings Symposium IEEE Photonics Society Benelux, pp. 128-131, 2017.
- [4] M. Fiers, T. Van Vaerenbergh, K. Caluwaerts, D. Vande Ginste, B. Schrauwen, J. Dambre, and P. Bienstman, "Time-domain and frequency-domain modeling of nonlinear optical components on circuit-level using a node-based approach," J. Opt. Soc. Am. pp. 82-900, 2012.